# Design and construction of CanSat educational satellites

# Diseño y construcción de satélites educativos CanSat

ORTEGA-ALVAREZ, Eduardo†*, HERNÁNDEZ-TORRES, Martha, ALVARADO-ANTÚNEZ, José Alfredo and GÓMEZ-ROA, Antonio

*Instituto Politécnico Nacional, México.*
*Universidad Autónoma de Baja California, México.*

ID 1st Author: *Eduardo, Ortega-Alvarez* / **ORC ID:** 0000-0002-3142-360X

ID 1st Co-author: *Martha, Hernández-Torres* / **ORC ID:** 0000-0003-3490-8255

ID 2nd Co-author: *José Alfredo, Alvarado-Antúnez* / **ORC ID**: 0009-0004-2258-7452

ID 3rd Co-author: *Antonio, Gómez-Roa* / **ORC ID:** 0000-0002-3548-0740, **CVU CONAHCYT ID:** 395899

**DOI:** 10.35429/P.2023.1.1.16



* eortegaa1500@alumno.ipn.mx

Á. Marroquín, L. Castillo, J. Olivares and A. Álvarez (AA. VV.). Young Researchers. Engineering Applications - Proceedings-©ECORFAN-México, Queretaro, 2023.

**Abstract**

Artificial satellites play a key role in research and modern communications serving the purpose of gathering data and transmitting it back to Earth. However, due to its complexity and strict quality standards, the design and construction of a satellite can span up to six years, making it challenging to teach this process to university students. Which is why the development of pico-satellites like CanSats provides students with the opportunity to learn the operation and basic systems of a satellite and their common launch vehicles on a small scale and in a short period of time. This paper explains the design and manufacturing process of a CanSat and a model rocket and their launch in the Mexican desert to gather data on the atmosphere throughout its descent, including height, pressure, air quality, latitude, and longitude. Additionally, it gives a brief explanation of the interface and database using Lab VIEW and Excel to plot all the collected variables.

**Satellite, CanSat, Launch vehicle, Model rockets, Data, Atmosphere, Complexity, Variables, Systems, Communications, Standards, Creation, Drones, Latitude**

**Resumen**

Los satélites artificiales juegan un importante papel en la investigación y las comunicaciones modernas, sirviendo el propósito de recolectar datos y enviarlos de vuelta a la Tierra. Sin embargo, debido a su complejidad y estrictos estándares de calidad, el desarrollo de un satélite puede durar hasta seis años, lo que dificulta enseñar este proceso a estudiantes universitarios. Es por eso por lo que el desarrollo de pico-satélites como CanSats brinda a los estudiantes la oportunidad de aprender el funcionamiento y los sistemas básicos de un satélite y sus vehículos de lanzamiento comunes a pequeña escala y en un corto periodo de tiempo. Este artículo describe cómo se construyeron un modelo de cohete y un CanSat y cómo se lanzaron en el desierto mexicano para recopilar datos sobre la atmósfera a lo largo de su descenso, incluida la altura, la presión, la calidad del aire, la latitud y la longitud. Adicionalmente, proporciona una breve explicación de la interfaz y la base de datos usando LabVIEW y Excel para graficar todas las variables.

**Satélite, CanSat, Vehículo de lanzamiento, Cohete modelo, Datos, Atmósfera, Complejidad, Variables, Sistemas, Comunicaciones, Estándares, Creación, Drones, Latitud**

## 1.1 Introduction

Artificial satellites hold significant importance in today's world. The main objective of these systems is data collection and signal transmission while placed in Earth orbit. Nonetheless, due to their remote location, providing maintenance and addressing repair issues is an arduous and unfeasible task. Hence, in their design, they must be able to withstand extreme temperatures, guarantee their survival in the case of space debris impact, and have a useful life of at least fifteen years (Maral, Bousquet, & Sun, 2020).

Given its complexity and intricate nature, the manufacturing of a satellite typically requires around six years, posing challenges for its incorporation into university-level education. For this reason, the development of a pico-satellite such as a CanSat represents an easily accessible option that enables students to acquire hands-on experience in conducting a space project. They can choose their mission objectives, design and integrate subsystems, prepare for a launch and collect, analyze and process the gathered data, all within a short period of time.

A CanSat (Can-Satellite) is a pico-satellite with dimensions like those of a 350 ml soda can and a weight of under 350 grams. Because of its small scale and weight, its primary purpose is to provide students with an opportunity to acquire fundamental concepts related to the design and construction of pico-satellites. Professor Robert Twiggs from Stanford University first proposed the CanSat project during the University Space Systems Symposium (USSS) held in Hawaii in November 1998.

Opposed to traditional satellites, CanSats typically function within the Earth's atmosphere and their release altitude varies depending on the mission goals. Along this descent trajectory, they execute specific missions, which usually involve tasks such as capturing images and/or video, collecting stored data, or transmitting information to an Earth station, among other functions. (University Space Engineering Consortium (UNISEC), 2017). In order to meet mission requirements, the CanSat system needs to be divided into distinct subsystems. Figure 1.1 provides a visualization of the CanSat's subsystems.

**Figure 1.1** Main subsystems of a CanSat

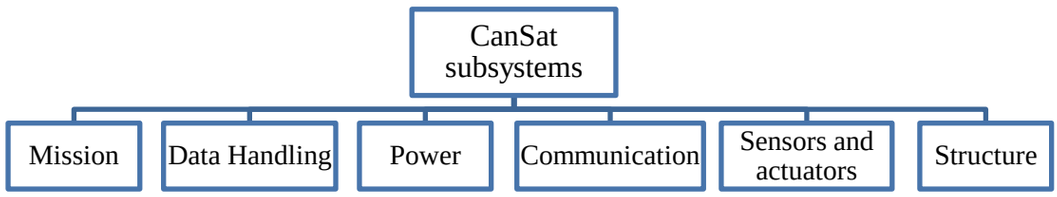


*Source: Own elaboration*

The Mission subsystem holds significant importance, as it defines the main objective of the CanSat during both launch and descent, it also communicates the intended investigation, measurement, capture, observation, or analysis. Therefore, it becomes essential to establish three success criteria: minimal, medium, and complete success. Determining the mission involves considering factors based on feasibility and available resources, such as tools, laboratories, test systems, experience levels, components, in addition to the constraints commonly imposed in competitions, like cost, dimensions, energy consumption, weight, atmospheric variables, and more. The command and data subsystem relies on physical components that facilitate the deployment of data at the software level of picosatellite operation. It comprises a flight computer that presents collected data through an interface, a data reception system, and, in some instances, the transmission of commands. The power subsystem focuses on providing the energy requirements to the system in compliance with a power budget depending on the different modes of operation. The main components are usually controllers, switches, power sources such as photovoltaic cells and batteries. The communication subsystem consists of a receiver, transmitter, channel, antenna, and communication protocol. In summary, it enables the transmission and reception of data or commands essential for the mission. It aids in understanding the operational status and recovery point of the CanSat. The attributes of internal components, such as weight, dimensions, temperature, humidity, current, and radio wave permeability, establish the materials, volume, and dimensions of the CanSat structure responsible for carrying them throughout the mission. (Agencia Espacial Mexicana (AEM), 2018)

Currently, the launch system is not only based on high-powered model rockets, other alternatives for launch vehicles are also weather balloons, model aircraft and quad copters. The type of launch device is dependent on factors such as the mission, height, weather conditions, and structure. Table 1.1 gives a description of some of the common launch devices used for pico-satellites.

**Table 1.1** Typical launch devices for CanSat

| Launch device | Description |
|---|---|
| Rocket model | It is a scale rocket made of lightweight and heat resistant materials that uses an engine of a liquid or solid fuel to be propelled during launch. The classification of the engine is based on the thrust it provides to the rocket. |
| Weather balloons | These latex or synthetic rubber balloons are inflated with hydrogen or helium. For CanSats, they are launched to attain a minimum height of 200 meters and a maximum of 4000 meters, ensuring the maintenance of stable and optimal conditions during ascent. |
| Model Aircraft. | Small scale aircraft consisting of a transmitter, receiver and servos, the maximum flight height is dependent on the range of the radio signal. |
| Quadcopters | Multi-rotor capable of lifting and propelling with 4 rotors, 2 rotating clockwise and the other pair counterclockwise. |

*Source: Own elaboration*

This article explains the process of designing and constructing a CanSat, along with detailing the model rocket employed for launch. To begin with, Section 1.2 describes the mission and main goals, as well as the Concept of Operation. Subsequently, Section 1.3 gives details about the characteristics of the BME680, NEO-7M, MQ-135, GY-91 sensors, which measure altitude, temperature, pressure, latitude, longitude, acceleration, position, among other atmospheric variables. Moving on to Section 1.4, it shows the communication subsystem and the main properties of the transceivers, such as their frequency and protocol. Transitioning to Section 1.5, it addresses the programming and integration of the microcontroller with the sensors. In Section 1.6, it illustrates the connection diagram for the electronic components, and Section 1.7 explains their physical integration to fit within the structure of the pico-satellite. Turning attention to Section 1.8, the article provides an explanation of the structure, the materials employed, and the underlying reasons for its architecture. Transitioning to Section 1.9, it details the design and manufacturing of the launch vehicle. Lastly, Section 1.10 elaborates on the process of development of the interface. Finally, the article gives a brief explanation of the results and conclusions of the project.

### 1.2 Mission objectives, success criteria and concept of operation

To achieve a comprehensive project perspective and maximize the likelihood of success, it is important to apply the principles of Systems Engineering throughout the development process. Different approaches exist for depicting and planning project lifecycles. The approach adopted for this project's development utilizes the V Model, as illustrated in Figure 1.2.

**Figure 1.2** V-model in systems engineering

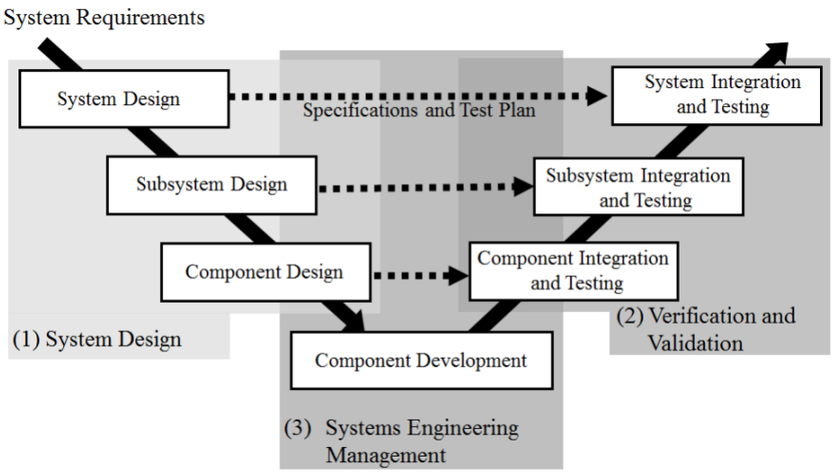


*Source: (University Space Engineering Consortium (UNISEC), 2017)*

The initial stage of project development involves defining the mission objectives and three success criteria: minimum success, medium success, and full success.

First, the mission objectives are defined. These objectives are to reach a height of 500 meters, release the CanSat to begin the descent and collect data, and process and transmit atmospheric readings from sensors to the ground base.

Second, the three success criteria are defined. The minimum success criteria is to reach a height of 500 meters, release the CanSat from the lifting device, and successfully deploy the parachute. The medium success criteria is to begin taking atmospheric readings periodically upon descent, transmit readings to ground base, and retrieve the CanSat. The full success criteria is to obtain readings with true data, useful evidence, and preserve the integrity of the CanSat upon recovery.

The Concept of Operation is illustrated in Figure 1.3 and it is described as follows:

- First, the CanSat is energized, initiating data transmission.
- Next, it is mounted onto the lifting device, which in this instance is a model rocket.

- Then, the CanSat is elevated to a height of 500 meters and deployed at its peak altitude.

- At this point, the parachute is deployed, initiating the descent phase. The ground computer receives transmitted data from the CanSat throughout its descent. The CanSat lands safely.

- Finally, the coordinates of the final recorded position are verified. The CanSat is retrieved and the collected data is analyzed.

**Figure 1.3** Concept of operation

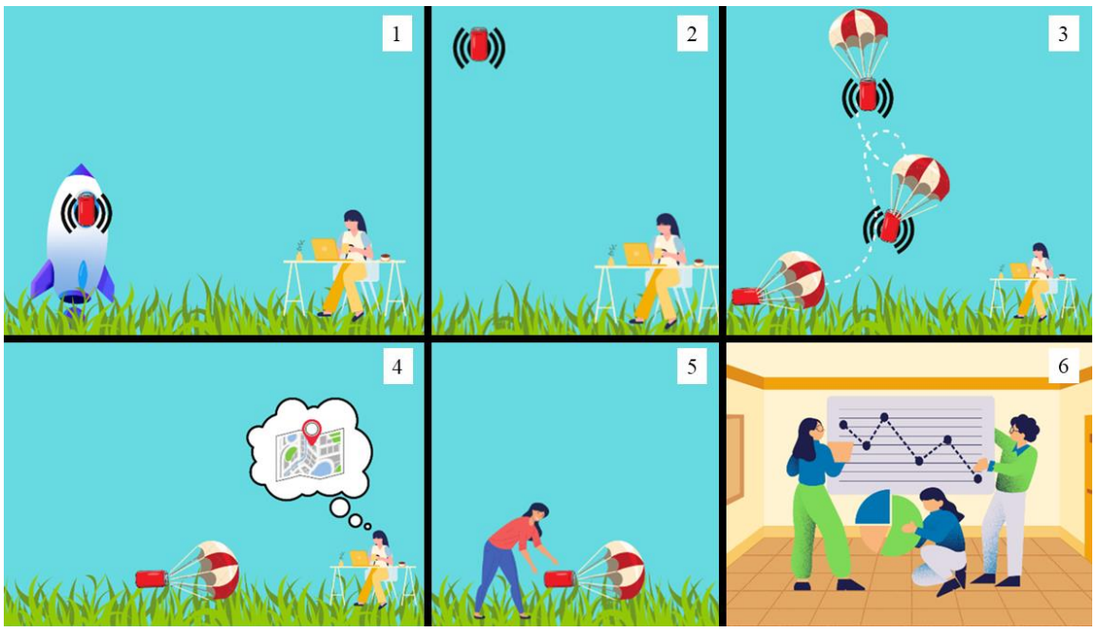


*Source: Own elaboration*

### 1.3 Sensors

The pico-satellite's mission requirements dictated the selection of its sensors, including the NEO-7M, GY-91, BME-680, and MQ-135. These sensors measure a range of atmospheric parameters, such as air quality, atmospheric pressure, humidity, altitude, latitude, orientation, acceleration, and magnetic fields. The following sections provide the main features and characteristics of each sensor.

#### 1.3.1 BME680

The BME6880 is a sensor that can measure air quality by integrating the measurement of several atmospheric variables, such as gas, humidity, relative humidity, barometric pressure, air quality, and temperature from -40 °C to 85 °C. It offers several advantages, including its compact size, low power consumption, stability, and strong electromagnetic compatibility performance. (Bosch Sensortec GmbH, 2022).

In addition, the device can identify a broad spectrum of gases, primarily volatile organic compounds (VOCs), by absorbing them into its sensitive layer of metal oxide. The sensor reacts to most VOCs and other pollutants and can measure their cumulative presence in the surrounding air. The sensor displays the VOC values using the Air Quality Index (AQI), which ranges from 0 (clean air) to 500 (very polluted air). Table 1.2 shows the AQI values and their corresponding descriptions based on the air quality scale (Secretaría del Medio Ambiente, 2018).

Finally, the most common uses of the sensor are to measure and indicate air quality and well-being in indoor environments.

**Table 1.2** Air quality classification index and color coding

| Index Value | Classsification | Precautions to protect yourself from ozone |
|---|---|---|
| 0 – 50 | Good | None |
| 51 – 100 | Moderate | Extremely sensitive individuals should consider limiting prolonged exertion outdoors. |
| 101 – 150 | Harmful to the health of sensitive groups | The elderly, children, active adults, and people with respiratory conditions such as asthma should avoid prolonged outdoor exertion and the rest of the population should limit their exposure. |
| 151 – 200 | Harmful to health | The elderly, children and people with respiratory diseases should avoid prolonged exertion in the open air and the rest of the population should limit their exposure. |
| 201 – 300 | Very harmful to health. | The entire population should avoid any outdoor effort. |

*Source: (Secretaría del Medio Ambiente, 2018)*

The BME680 pin configuration is illustrated in Figure 4. The following are the pin descriptions:

- VCC: The supply voltage pin, which provides power to the sensor. The voltage range is 3.3-5 VDC.
- GND: The ground pin, which provides a common reference for all the signals.
- SCL: The clock pin, which is used to synchronize the data transfer between the sensor and the microcontroller. The SCL pin can be used with both the I2C and SPI protocols.
- SDA: The data pin, which is used to transmit and receive data between the sensor and the microcontroller. The SDA pin can be used with both the I2C and SPI protocols.
- SDO: The serial data output pin, which is used to transmit data from the sensor to the microcontroller. The SDO pin is only used with the SPI protocol.
- CS: The chip select pin, which is used to select the BME680 chip when communicating with multiple sensors. The CS pin is only used with the SPI protocol.

**Figure 1.4** BME680 sensor module

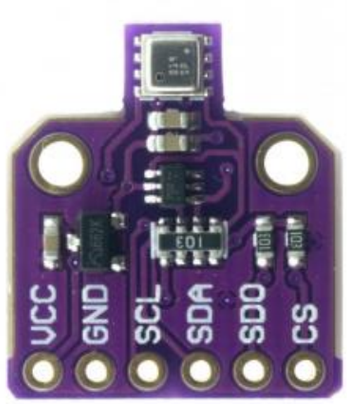


*Source: (Bosch Sensortec GmbH, 2022)*

### 1.3.2 NEO-7M

The NEO-7M is a GNSS (Global Navigation Satellite Systems) module that provides GPS satellite positioning. Moreover, its main features are high sensitivity with a maximum navigation update rate of 10 Hz. Additionally, it boasts high integration capacity in a compact system and great synergy between its elements. Furthermore, the module chips are certified, providing reliability, which is an important aspect of their choice in the project. (u-blox, 2014). The module has four pins: VCC, GND, TXD, and RXD that are shown in Figure 1.5 and are described below (techmake, 2022):

- VCC is the power supply pin, which provides 3.3V to 5V power to the module.
- GND is the ground pin, which provides a common reference voltage for the module.
- TXD is the serial port transmission pin, which is used to transmit data from the module to the microcontroller.
- RXD is the serial port receive pin, which is used to receive data from the microcontroller.

**Figure 1.5** NEO-7M module


*Source:(techmake, 2022)*

### 1.3.3 MQ-135

The MQ-135, an electrochemical air quality sensor that changes its resistance in response to different chemical compounds in the air, offers versatile capabilities. Notably, it can detect ammonia (NH3), nitrogen oxides (NOx), alcohol, benzene (C6H6), smoke, carbon dioxide (CO2), sulfides, carbon monoxide (CO), and other harmful gases.

This module measures hazardous gases in parts per million (ppm), making it a valuable tool for air quality assessment. Its wide detection range of 10 to 1000 ppm makes it suitable for integration into air quality management systems across various settings, including residences, commercial buildings, offices, and industrial facilities dealing with hazardous gases. Additionally, the sensor operates effectively between -20 °C and 70 °C, ensuring reliable performance even in diverse environmental conditions. Remarkably, it weighs only 8 grams, enhancing its portability and ease of use.

In the specific project context, the MQ-135 was employed to record the air quality variable, which was quantified at ppm, demonstrating its adaptability and relevance for air quality monitoring.

The MQ-135 gas sensor has four connection pins, as shown n Figure 1.6 These pins are described below:

- Vcc: This pin is used to power the sensor. The operating voltage is typically 5V.
- Ground: This pin is used to connect the sensor to the system ground or reference.
- Digital output: This pin can be used to obtain a digital output from the sensor. The threshold value for the digital output can be set using the potentiometer.
- Analog output: This pin outputs an analog voltage of 0-5V, depending on the intensity of the gas.

**Figure 1.6** MQ-135 module

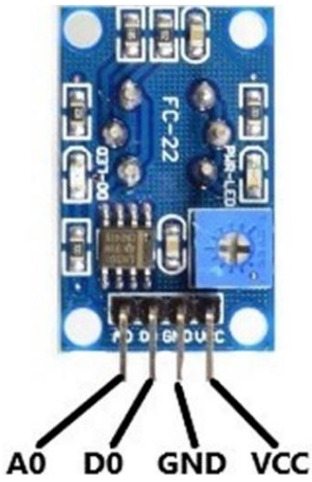


*Source: (Nawazi, 2021)*

### 1.3.4 GY-91

The GY-91 module incorporates two sensors, the IMU MPU9250 and the BMP280. The system integrates 10 degrees of freedom, which are manifested as a 3-axis gyroscope, a 3-axis accelerometer, a 3-axis magnetometer, and an altimeter. In addition, the implementation allowed for the acquisition of data from the gyroscope, accelerometer, temperature, pressure, and altitude. (Zago, 2017)

The IMU MPU9250 has a digital motion processor that accurately captures the fast and slow movements of 9 axes using complex algorithms. It has a programmable scale range of 250/500/1000/2000 degrees/s for the gyroscope, 2g/4g/8g/16g for the accelerometer, and ±4800μT for the magnetometer.

Furthermore, the BMP280 is a barometric pressure sensor that is known for its exceptional accuracy and minimal power consumption. It operates within a range of 300 to 1100 hPa and offers impressive precision, linearity, long-term stability, high pressure resolution, high precision temperature, and digital filters. (Mechatronics, 2019).

The connection pins of the GY-91 are shown in Figure 1.7. They are described below:

- VIN: This pin supplies the GY-91 with 5V power.
- 3V3: This pin outputs 3.3V power.
- GND: This pin is the ground pin.
- SCL: This pin is the clock pin for the I2C and SPI protocols.
- SDA: This pin is the data pin for the I2C and SPI protocols.
- NCS: This pin is used to select the MPU-9250 chip when using the SPI protocol.
- CSB: This pin is used to select the BMP280 chip.

**Figure 1.7** GY-91 module

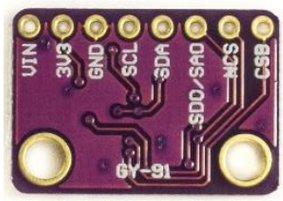


*Reference source: (Mechatronics, 2019)*

### 1.4 Communication subsystem

Figure 1.8 showcases the XBee, a radio module utilized for establishing wireless connectivity among various devices. When implemented in the picosatellite, this module enables both data transmission and reception functionalities. The XBee module actively employs the IEEE 802.15.4 protocol operating at a frequency of 2.4Hz. This protocol facilitates the creation of either point-to-multipoint or point-to-point networks. These modules are particularly suited for applications demanding high data traffic, low latency, and precise communication timing. The module itself incorporates a reception and emission system for wireless data operation, commonly referred to as the coordinator and router (Digikey, 2009).

**Figure 1.8** XBee module


*Source: (Digikey, 2009)*

For configuring, testing, and visualizing data on the XBee module, users typically turn to the cross-platform application known as XCTU. XCTU equips users with the essential tools needed for the effective operation of the XBee module. The primary objective behind the integration of the XBee module was to enable the wireless transmission of data collected from the sensors to a designated device, such as a computer.

### 1.5 Microcontroller

The pico-satellite uses the Arduino Nano microcontroller, as depicted in Figure 1.9. This electronic board measures 45mm x 18mm and is a practical choice given the size and weight constraints of the CanSat. It features an ATmega328P microchip and has 14 digital pins, 8 analog pins, 2 reset pins, and 6 power pins, offering similar power and connectivity capabilities as the Arduino Uno. The Arduino Nano also has a Mini-USB connector, Jack connector, and different header pins. It is worth noting that the Arduino Nano has the same memory space compared to the Arduino Uno. However, the Arduino Nano microcontroller is more than adequate to fulfill the memory requirements of the mission, which primarily focuses on data collection (Arduino, 2021).

**Figure 1.9** Arduino Nano

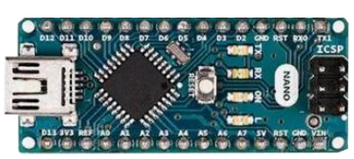


*Source: (Arduino, 2021)*

### 1.6 Electrical connections between modules

A proactive strategy was used to design the system integration of the CanSat, considering the individual descriptions of the sensor modules and the data transmission and reception components. This promoted seamless interaction. Figure 1.10 illustrates the schematic layout of the electrical connection network. The Arduino Nano Microcontroller was used to link all sensors and the XBee RF module, which facilitated programming.

**Figure 1.10** Electrical connections of the wireless modules and sensors of the CanSat

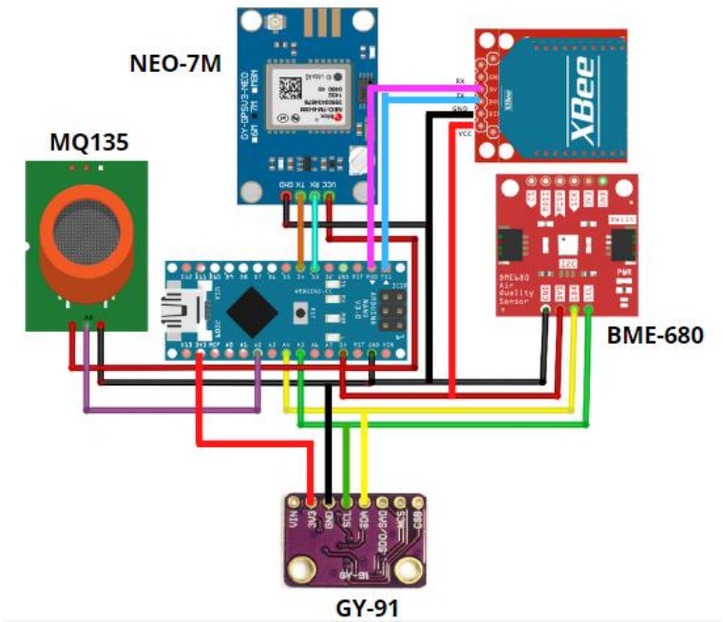


*Source: Own elaboration. Fritzing v.0.9.3*

### 1.7 Physical integration of electronic components

The physical integration of the components was made using a perforated board, as shown in Figure 1-11. The perforated board is ideal for this application as it already has pre-drilled holes which makes it easy to mount the components. The image shows the 12V Lipo battery as well, which is used to energize the system. The battery is connected to the Arduino Nano Microcontroller, which controls the operation of the sensors and the XBee RF module. The perforated board is an essential part of the CanSat, as it allows for the efficient and secure integration of all the components.

**Figure 1.11** Integration of the sensors, microcontroller, battery and RF module in a perforated board

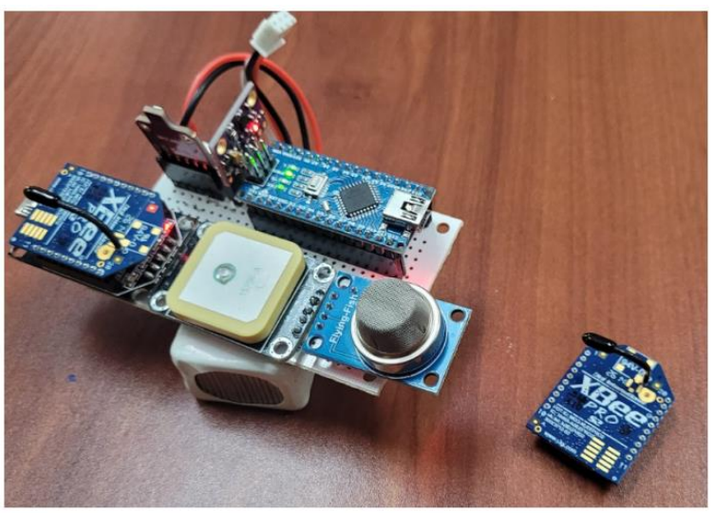

*Source: Own elaboration*

## 1.8 Structural subsystem

To facilitate the construction of the picosatellite, the utilization of PLA (polylactic acid) is essential. This material includes a slot for the insertion of a perforated card containing electronic components. In addition, the structural design incorporates a rectangular cavity specifically designed to accommodate the lithium polymer battery responsible for powering the system. Notably, for optimization, this structural model also integrates strategically placed holes within the external wall to effectively reduce weight (Figure 1.12).

**Figure 1.12** PLA container used for the structural subsystem

*Source: Own elaboration*

## 1.9 Launch vehicle

A launch vehicle assumes the responsibility of elevating the CanSat to a designated altitude and initiating its deployment. During the CanSat's development, a model rocket was designated to fulfill the role of the launch vehicle.

During the development of the CanSat, a model rocket was selected to serve as the launch vehicle. Model rockets are made of cardboard or fiberglass and have fins made of plastic, wood, cardboard, or fiberglass. The rocket's engine can be purchased commercially or made individually and can be disposable or reusable. The engine is fitted snugly within the engine mount, which transfers the thrust generated by the engine to the rocket's body. The upper segment of the engine houses the ejection charge, which is responsible for expelling the nose cone, recovery system, and payload. The recovery system helps to slow down the rocket's descent and typically uses a parachute. The payload is the CanSat itself. The nose cone is attached to the engine mount by a shock cord that must withstand the force from the ejection charge. Launch lugs are affixed along the rocket body's sides to secure the rocket to the launch rail. Figure 1.13 shows a visual representation of each component of a model rocket (Benson, 2021).

**Figure 1.13** Parts of a model rocket. 1. Body of the rocket. 2. Fins. 3. Engine mount. 4. Washers to adjust engine. 5. Engine. 6. Engine explosive charge. 7. Nose cone. 8. Recovery system. 9. Payload. 10. Shock cord. 11. Rails of the rocket

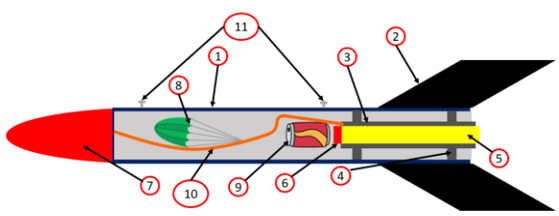


*Source: (Benson, 2021).*

The rocket was designed using the OpenRocket software, a freely available program dedicated to model rocket design. This software allows users to distribute the weights of rocket components, specify the type of fins, and select the preferred engine brand. Figure 1.14 shows a CAD model of the rocket.

**Figure 1.14** CAD model of the developed rocket

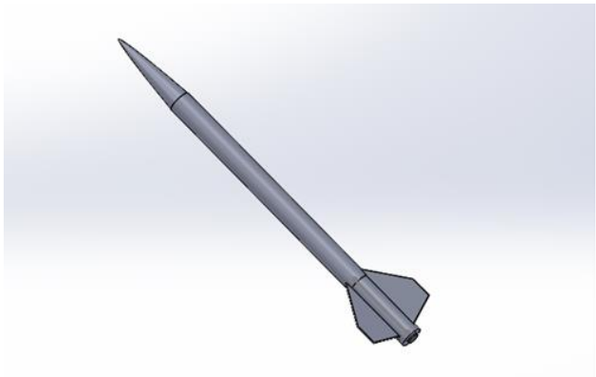

*Source: Own elaboration. Solid Works, 2022*

The rocket's construction involves the process of adhering layers of fiberglass with epoxy. To construct the rocket, fiberglass was applied to a PVC tube with the desired diameter, which had been enveloped in waxed paper. This allowed the fiberglass to be easily released. Flat components were then cut using band saws and jigsaws. These components were then refined to achieve the desired dimensions through sanding. The nose cone of the rocket was shaped using an existing mold. Figure 1.15 shows a visual representation of the manufacturing process.

**Figure 1.15** Model rocket manufacturing process. From left to right: Applying epoxy to fiberglass in order to manufacture fins of the rocket. Cutting the fiberglass to the desired form. Body of the rocket. Rocket fully painted

*Source: Own elaboration.*

## 1.10 Interface

To visualize and store the collected data from the sensors, an interface was created within LabVIEW. This environment is widely utilized in academic contexts for its user-friendly block programming approach, enabling the creation of graphical interfaces without the need for written code. Additionally, its extensive library collection facilitates the execution of a wide variety of functions. The data collected by the sensors is sent via serial communication by the XBEE module. This data is structured in a text line format and separated by semicolons, destined for the ground computer. LabVIEW interacts with the serial module through the I/O library. It categorizes the data based on variable names and presents it numerically on the interface, as well as plots it graphically. Additionally, LabVIEW displays the recorded timestamps for data transmission from the NEO-7M sensor and the time of reading by the computer, facilitating a comparison of the time delay between these two instances. For further examination, the data is stored in an Excel spreadsheet within the Microsoft Office suite.

**Figure 1.16** Graphic interface developed in LabVIEW

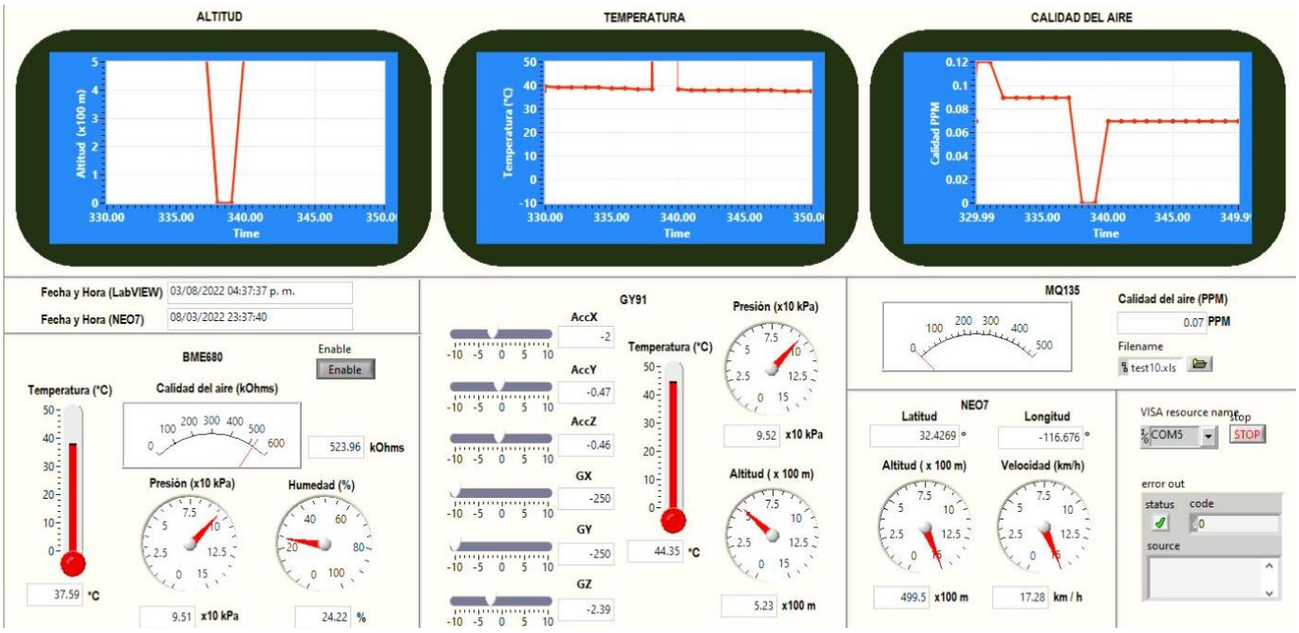


*Source: Own elaboration. LabVIEW, 2021*

**Figure 1.17** Data collected and stored in Excel

| | A | B | C | D | E | F | G | H | I | J | K | L | M | N | O | P |
|---|---|---|---|---|---|---|---|---|---|---|---|---|---|---|---|---|
| 1 | Time | Temperatura BME680 | Presión kPa BME680 | Humedad % BME680 | Calidad del aire kOhms BME680 | AccX GY-91 | AccY GY-91 | AccZ GY-91 | GX GY-91 | GY GY-91 | GZ GY-91 | Altitud x100m GY-91 | Presión kPa GY-91 | Temperatura GY-91 | Calidad aire MQ135 | Latitud NEO-7 |
| 2 | 03/08/2022 16:23:49.073 | 0 | 0 | 0 | 0 | 0 | 0 | 0 | 0 | 0 | 0 | 0 | 0 | 0 | 0 | 0 |
| 3 | 03/08/2022 16:23:50.073 | 36 | 9.77 | 30.26 | 309.02 | -2 | -0.46 | 0.3 | 16.01 | 36.98 | -2.33 | 3.11 | 9.76 | 36.95 | 0.02 | 0 |
| 4 | 03/08/2022 16:23:51.074 | 35.95 | 9.77 | 30.28 | 309.02 | -2 | -0.41 | -0.06 | -18.04 | 1.56 | -2.17 | 3.11 | 9.76 | 36.97 | 0.02 | 0 |
| 5 | 03/08/2022 16:23:52.074 | 35.94 | 9.77 | 30.37 | 308.93 | -2 | -0.46 | 0.06 | -14.83 | -6.67 | -2.31 | 3.11 | 9.76 | 36.98 | 0.02 | 0 |
| 6 | 03/08/2022 16:23:53.074 | 35.94 | 9.77 | 30.44 | 308.85 | -2 | -0.66 | 0.11 | 9.16 | -7.45 | -2.22 | 3.11 | 9.76 | 37.03 | 0.02 | 0 |
| 7 | 03/08/2022 16:23:54.074 | 35.94 | 9.77 | 30.56 | 308.93 | -2 | -0.72 | 0.04 | -2.66 | -12.66 | -2.29 | 3.11 | 9.76 | 37.1 | 0.02 | 0 |
| 8 | 03/08/2022 16:23:55.712 | 35.96 | 9.77 | 30.61 | 308.93 | -2 | -0.73 | 0.09 | -5.09 | -9.73 | -2.25 | 3.11 | 9.76 | 37.13 | 0.02 | 0 |
| 9 | 03/08/2022 16:23:58.027 | 35.98 | 9.77 | 30.62 | 309.02 | -2 | -0.78 | 0.06 | -3.86 | -3.12 | -2.24 | 3.11 | 9.76 | 37.19 | 0.02 | 0 |
| 10 | 03/08/2022 16:24:00.296 | 35.97 | 9.77 | 30.62 | 309.02 | -2 | -0.73 | 0.07 | -3.34 | -5.91 | -2.3 | 3.11 | 9.76 | 37.23 | 0.02 | 0 |
| 11 | 03/08/2022 16:24:02.690 | 35.99 | 9.77 | 30.6 | 308.93 | -2 | -0.83 | 0.01 | 12.17 | -8.79 | -2.43 | 3.11 | 9.76 | 37.23 | 0.02 | 0 |
| 12 | 03/08/2022 16:24:05.020 | 35.99 | 9.77 | 30.58 | 308.85 | -2 | -0.81 | 0.08 | 0.76 | -6.98 | -2.43 | 3.11 | 9.76 | 37.24 | 0.02 | 0 |
| 13 | 03/08/2022 16:24:07.289 | 35.97 | 9.77 | 30.68 | 308.85 | -2 | -0.78 | 0.08 | -1.22 | -1.32 | -2.35 | 3.11 | 9.76 | 37.31 | 0.02 | 0 |
| 14 | 03/08/2022 16:24:09.714 | 35.99 | 9.77 | 30.66 | 308.93 | -2 | -0.84 | 0.19 | 12.79 | -49.95 | -2.29 | 3.12 | 9.76 | 37.36 | 0.02 | 0 |
| 15 | 03/08/2022 16:24:12.046 | 36 | 9.77 | 30.71 | 308.93 | -2 | -0.85 | -0.44 | 10.83 | 1.35 | -2.24 | 3.11 | 9.76 | 37.4 | 0.02 | 0 |
| 16 | 03/08/2022 16:24:14.298 | 35.99 | 9.77 | 30.56 | 308.93 | -2 | -0.84 | -0.23 | -22.77 | -20.03 | -2.36 | 3.12 | 9.76 | 37.44 | 0.02 | 0 |
| 17 | 03/08/2022 16:24:16.724 | 36.02 | 9.77 | 30.47 | 308.85 | -2 | -0.85 | -0.32 | 5.62 | -9.57 | -2.32 | 3.11 | 9.76 | 37.39 | 0.02 | 0 |
| 18 | 03/08/2022 16:24:19.055 | 36.05 | 9.77 | 30.4 | 308.85 | -2 | -0.63 | -0.64 | -3.78 | -11.65 | -2.33 | 3.11 | 9.76 | 37.43 | 0.02 | 0 |
| 19 | 03/08/2022 16:24:21.307 | 36.04 | 9.77 | 30.24 | 308.76 | -2 | -0.46 | -0.56 | 10.76 | -20.32 | -2.31 | 3.11 | 9.76 | 37.36 | 0.02 | 0 |
| 20 | 03/08/2022 16:24:23.702 | 36.05 | 9.77 | 30.25 | 308.85 | -2 | -0.41 | -0.56 | 10.8 | 5.49 | -2.34 | 3.12 | 9.76 | 37.38 | 0.02 | 0 |
| 21 | 03/08/2022 16:24:26.033 | 36.07 | 9.77 | 30.14 | 308.85 | -2 | -0.6 | -0.66 | 18.52 | -6.53 | -2.36 | 3.12 | 9.76 | 37.37 | 0.02 | 0 |
| 22 | 03/08/2022 16:24:28.284 | 36.04 | 9.77 | 30.35 | 308.93 | -2 | -0.69 | -0.24 | -10.65 | -58.9 | -2.2 | 3.12 | 9.76 | 37.42 | 0.02 | 0 |
| 23 | 03/08/2022 16:24:30.695 | 36.04 | 9.77 | 30.52 | 309.02 | -2 | -0.67 | -0.81 | -44.88 | -40.95 | -2.44 | 3.12 | 9.76 | 37.47 | 0.02 | 0 |
| 24 | 03/08/2022 16:24:33.025 | 36.01 | 9.77 | 30.47 | 309.11 | -2 | -0.61 | -0.76 | -0.76 | 2.5 | -2.38 | 3.12 | 9.76 | 37.39 | 0.02 | 0 |
| 25 | 03/08/2022 16:24:35.278 | 35.95 | 9.77 | 30.45 | 309.11 | -2 | -0.62 | -0.77 | 0.4 | -7.48 | -2.21 | 3.12 | 9.76 | 37.44 | 0.02 | 0 |
| 26 | 03/08/2022 16:24:37.703 | 35.88 | 9.77 | 30.3 | 309.02 | -2 | -0.59 | -0.8 | -0.25 | -7.61 | -2.42 | 3.11 | 9.76 | 37.43 | 0.02 | 0 |
| 27 | 03/08/2022 16:24:40.034 | 35.78 | 9.77 | 30.27 | 309.11 | -2 | -0.56 | -0.71 | 9.29 | -6.22 | -2.23 | 3.11 | 9.76 | 37.36 | 0.02 | 0 |

*Source: Own elaboration. Excel, Version 2304.*

## 1.11 Results

Using a level L2 engine, a launch was made for data collection through the CanSat. The result for each recorded variable is presented as follows:

### 1.11.1 Height

The maximum elevation recorded on the rocket was 583.8 m, from 310 mamsl at the launch site to 893.8 mamsl. The total flight time between launch and maximum height was 14 seconds, and the fuel of the rocket burned in 2 seconds. Graphic 1.1 illustrates the height reached versus the time recorded by the CanSat.

**Graphic 1.1** Altitude graph of the GY-91 and NEO-7M sensor on the CanSat during the mission and descent

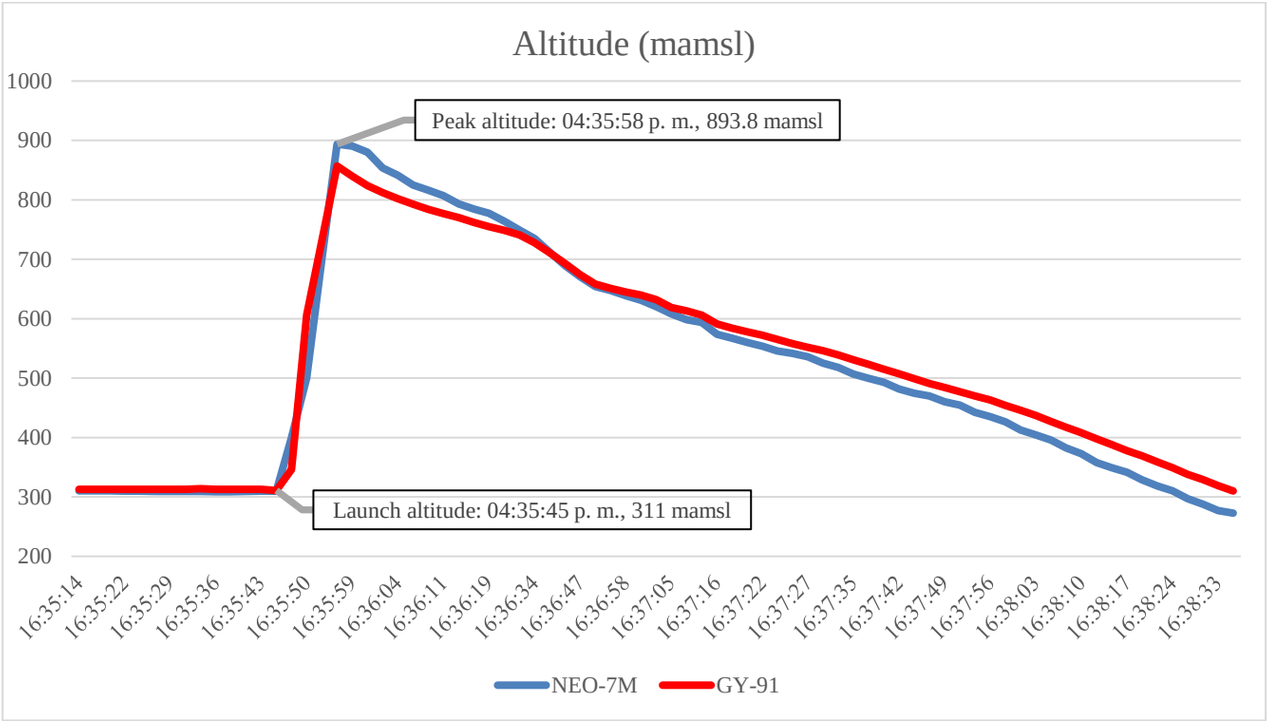


*Source: Own elaboration. Excel, 2021*

### 1.11.2 Pressure

The obtained data revealed a reduction in pressure as the rocket ascended. This phenomenon occurs due to the relationship between atmospheric pressure and the weight of the air column exerted on an object. As the altitude increases, the length of the air column decreases, resulting in a decreased amount and weight of air pressing on the object. Consequently, the overall pressure diminishes.

**Graphic 1.2** Pressure graph of the BME680 and NEO-7M sensor on the CanSat during the mission and parachute descent

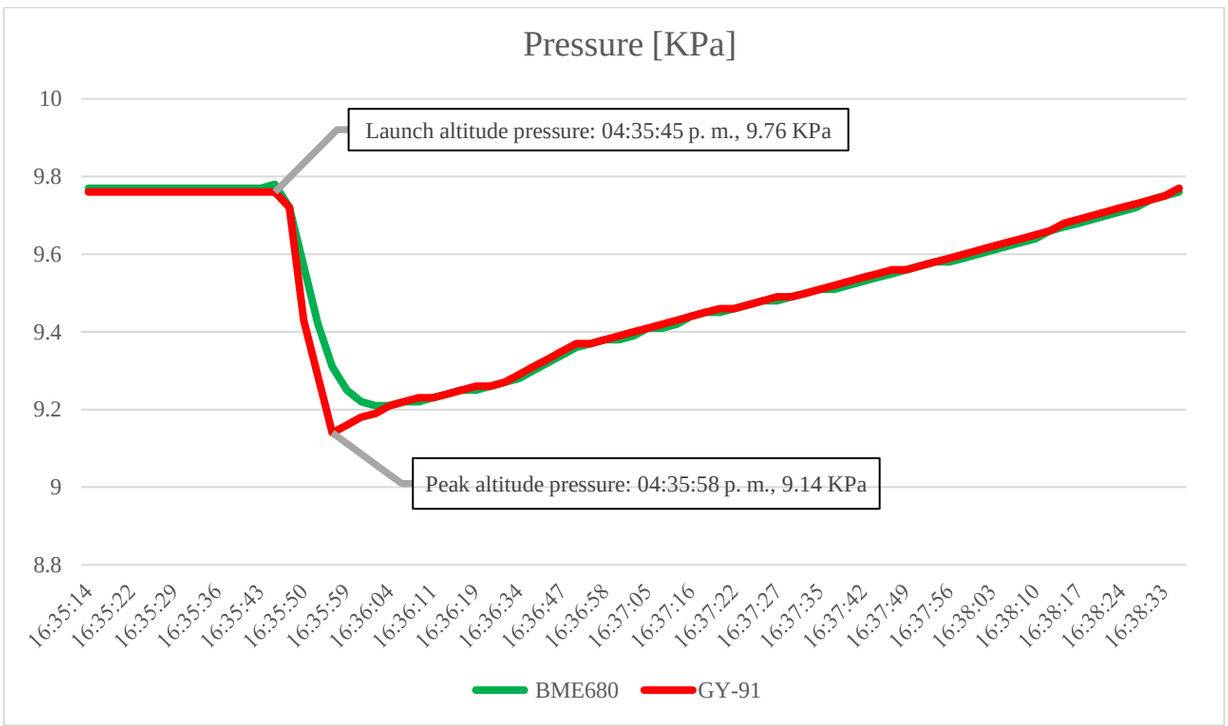


*Source: Own elaboration. Excel, 2021*

### 1.11.3 Humidity

The atmosphere contains water vapor, which is known as atmospheric humidity. The findings indicate a decline in atmospheric humidity as altitude increases. This phenomenon arises from the decrease in gas density within the concentrated atmospheric layers at higher altitudes, thereby limiting the atmosphere's water retention capacity.

**Graphic 1.3** CanSat humidity graph during the mission until the parachute descent

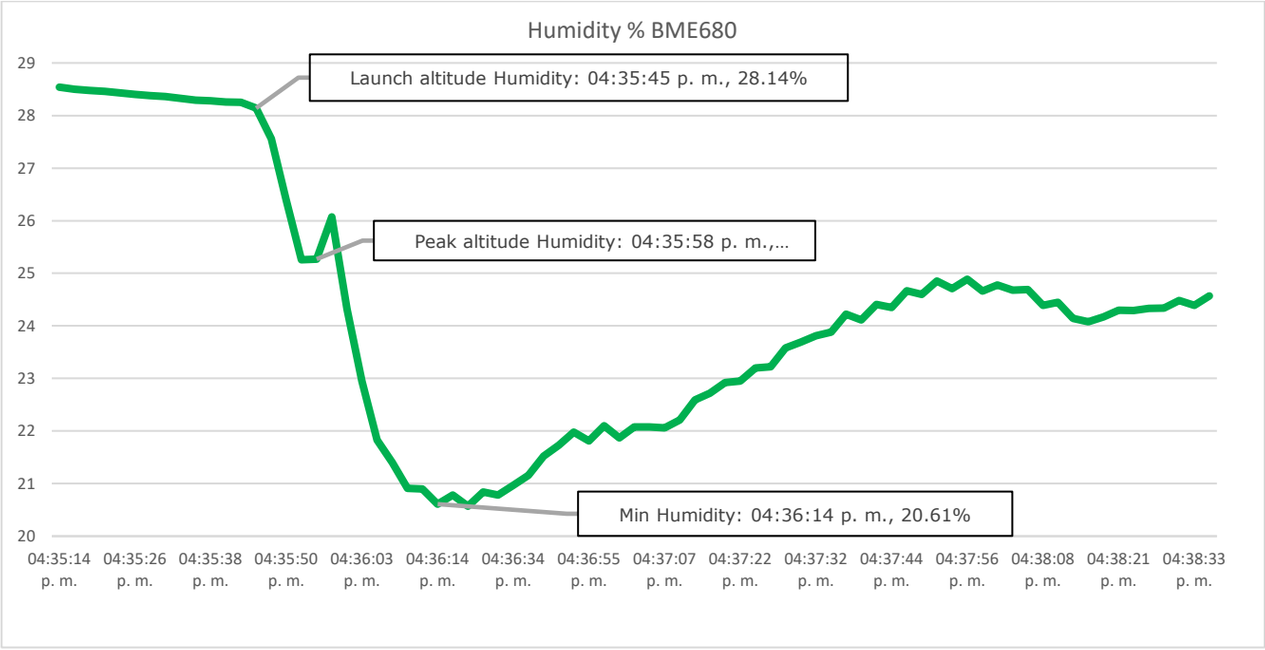


*Source: Own elaboration. Excel, 2021*

### 1.12 Conclusions

The developed picosatellite and launch vehicle met the mission objectives based on the described success evaluation, obtaining all the data of the required variables during the launch and complied with the mission criteria of full success. The development of these systems opens the possibility of participating in competitions where construction limitations are defined, such as volume, weight and data to be obtained. The mission was carefully defined, setting clear and specific objectives to measure key variables and better understand our atmospheric environment, as well as objectives related to payload and launch vehicle survivability.

The design and manufacturing process required a meticulous approach and careful planning. From the concept, the specific development, the simulation, the selection of materials and the tools used for its manufacture. The CanSat was designed with essential parts based on the main subsystems scheme, including the microcontroller, communications subsystem, height, pressure, temperature, acceleration, gyroscope, and air quality sensors. Additionally, a power budget was made according to the modes of operation for the selection of the battery. In the design of the structural system, mechanical supports were also considered to secure the parachute cords that would fulfill the task of the recovery system.

Through launch tests, the CanSat demonstrated its functionality and ability to measure previously defined variables. The height, pressure, temperature, acceleration, rotation, and air quality were recorded and transmitted via telemetry, providing valuable information about the atmospheric environment of Laguna Salada, Mexicali in the state of Baja California. In conclusion, the design and manufacturing process of a CanSat allows the development of a project that starts from the design of a mission, the analysis of a system to meet a certain weight, power and dimensions, the integration of subsystems, the generation of an environment that allows the reception and transmission of data that are essential to study and analyze the environment with which the CanSat interacts, thus also fostering interest in science and technology, promoting practical learning and exploration of aerospace topics.

**1.13 References**

Agencia Espacial Mexicana (AEM). (2018). *Ingeniería de Sistemas Espaciales. Aplicado a una misión CanSat.* Retrieved August 18, 2023, from Educación Espacial AEM: https://www.educacionespacial.aem.gob.mx/images_ise/pdf/05Sistemas%20Espaciales%20CanSat.pdf
Arduino. (2021). *Arduino Nano.* Ivrea. Retrieved from https://store.arduino.cc/products/arduino-nano

Benson, T. (2021, May 13). *Model Rockets*. Retrieved August 20, 2023, from NASA Glenn Research Center The Beginner's Guide to Aeronautics: https://www.grc.nasa.gov/www/k-12/rocket/rktparts.html

Bosch Sensortec GmbH. (2022, August). BME680 Low power gas, pressure, temperature & humidity sensor. *BME680 – Datasheet*. Kusterdingen, Baden-Württemberg, Germany: Bosch. Retrieved August 18, 2023, from https://www.bosch-sensortec.com/media/boschsensortec/downloads/datasheets/bst-bme680-ds001.pdf

Digikey, I. (2009). *Xbee /Xbee-PRO RF Modules.* USA: IEEE. Retrieved from https://www.sparkfun.com/datasheets/Wireless/Zigbee/XBee-Datasheet.pdf

Maral, G., Bousquet, M., & Sun, Z. (2020). *Satellite Communications Systems: Systems, Techniques and Technology* (6th ed.). Chichester, West Sussex, UK: John Wiley & Sons Ltd. doi:10.1002/9781119673811

Mechatronics, N. (2019). *Módulo GY-91* . Perú: SAC. Retrieved from https://naylampmechatronics.com/sensores-posicion-inerciales-gps/356-modulo-gy-91-mpu9250-bmp280-acelerometro-giroscopio-magnetometro-altimetro-i2c.html

Nawazi, F. (2021, October 30). *MQ135 Air Quality Smoke Gas Sensor Module*. Retrieved August 20, 2023, from Circuits DIY: https://www.circuits-diy.com/mq135-air-quality-smoke-gas-sensor/

Secretaría del Medio Ambiente. (2018, Noviembre 14). AVISO POR EL QUE SE DA A CONOCER LA NORMA AMBIENTAL PARA EL DISTRITO FEDERAL NADF009-AIRE-2017, QUE ESTABLECE LOS REQUISITOS PARA ELABORAR EL ÍNDICE DE CALIDAD DEL. *Gaceta Oficial de la Ciudad de México*(452). Retrieved August 19, 2023, from http://www.aire.cdmx.gob.mx/descargas/monitoreo/normatividad/NADF-009-AIRE-2017.pdf

techmake. (2022). *techmake*. Retrieved August 20, 2023, from Módulo GPS Ublox NEO-7M con Antena: https://techmake.com/products/gpsmod00563

u-blox. (2014, November 11). NEO-7 u-blox 7 GNSS modules. *Data Sheet(UBX-13003830)*. u-blox. Retrieved August 19, 2023, from https://content.u-blox.com/sites/default/files/products/documents/NEO-7_DataSheet_%28UBX-13003830%29.pdf

University Space Engineering Consortium (UNISEC). (2017). *CanSat Pico Size Artificial Satellite. A Guidebook for Building Successful CanSat Project.* Retrieved from http://unisec.jp/library/i-cansat/manual_CanSat_textbook_eng_v5.pdf

Zago, R. (2017). *GY91-MPU9250-BMP280.* Sao Paulo: GitHub. Retrieved from https://github.com/ricardozago/GY91-MPU9250-BMP280